Polymer Journal (2012) 44, 795–801

www.nature.com/pj

ORIGINAL ARTICLE

Solid-state ^{1}H-NMR relaxation behavior for ultra-high-molecular-weight polyethylene reactor powders with different morphologies

Hiroki Uehara, Hidekazu Tanaka and Takeshi Yamanobe

The relaxation behaviors of several commercial ultra-high-molecular-weight polyethylene (UHMW-PE) reactor powders were compared. The surface and internal morphologies of these powders were characterized by scanning and transmission electron microscopy observations. On the basis of these morphological analyses, the reactor powder consisted of particles and fibrils between them, the relative amounts of which depended on the powder preparation conditions. Molecular motions were detected by solid-state proton nuclear magnetic resonance (^{1}H-NMR) techniques. The temperature dependence of the molecular motion characterizes the structural differences between these powders. The intermediate region between crystal/amorphous phases first relaxes during gradual heating from room temperature for all reactor powders examined in this study. Such a release of constraint for boundary chains induces structural reorganization beyond the critical temperature before melting. This trend was also confirmed by an increase in crystallinity beyond the critical temperature. In contrast, the results of differential calorimetry (DSC) analysis could not distinguish these powder characteristics because of the remarkable reorganization of these reactor powders during heating scans. A relationship between the morphological and ^{1}H-NMR relaxation characteristics was interpreted for several reactor powders.
Polymer Journal (2012) **44,** 795–801; doi:10.1038/pj.2012.104; published online 13 June 2012

Keywords: morphology; reactor powder; solid-state NMR; ultra-high-molecular-weight polyethylene

INTRODUCTION

Semi-crystalline polymers have different morphologies, depending on their crystallization conditions. Solution crystallization often induces the regular stacking of lamellar crystals, and a typical spherulite structure is formed by crystallization from a melt. In contrast, crystallization during polymerization is quite different. Such crystallization is initiated immediately after the chain segments grow during polymerization.[1,2] This avoids molecular entanglement during reactor powder synthesis;[3–6] thus, ultra-drawing into the high-performance films is achieved for ultra-high-molecular-weight polyethylene (UHMW-PE).[7–10] Indeed, the drawability depends on the UHMW-PE reactor powders observed and determines the resultant material properties.[9] Among the commercially available UHMW-PE reactor powders, such as Hifax (Hercules), Hizex (Mitsui), SunFine (Asahi Kasei) and Hostalen (Ticona), one is drawable, but the others exhibit less ductility.[11] Therefore, the characterization of reactor powders is of interest in understanding the mechanism of crystallization during polymerization, and developing industrial applications for high-performance-film manufacturing.

There are several techniques used to characterize reactor powders. The most popular approach is microscopic observation using scanning electron microscopy (SEM) or transmission electron microscopy (TEM). The advantage of these microscopic observations is the direct recognition of different morphologies, depending on the powders studied. Indeed, PE reactor powders exhibit 'cobweb' structures composed of particles and fibrils.[9] However, the quantitative analyses for such characteristic morphologies in reactor powders are difficult, because these observations do not report any quantitative values. In contrast, X-ray or differential calorimetry (DSC) measurements can characterize the crystallinity of a powder. However, these methodologies focus on the crystalline components of materials; therefore, state of the noncrystalline component remains unclear, although the molecular entanglements are contained in noncrystalline phases. Thus, the characterization of the noncrystalline component is key in understanding the relationship between reactor powder morphology and drawability.

Nevertheless, there are a few techniques that allow for the characterization of noncrystalline phases. Nuclear magnetic resonance (NMR) is a possible candidate. The advantage of NMR analysis lies in its simultaneous monitoring of noncrystalline phases as well as crystalline phases; thus, the comparison of their characteristics is possible. This is quite different from other analytical techniques. Indeed, we have analyzed UHMW-PE samples prepared under different conditions, including the as-polymerized reactor powder

Department of Chemistry and Chemical Biology, Gunma University, Kiryu, Japan
Correspondence: Professor H Uehara, Department of Chemistry and Chemical Biology, Gunma University, 1-5-1 Tenjin-cho, Kiryu, Gunma 376-8515, Japan.
E-mail: hirokiuehara@gunma-u.ac.jp
Received 26 January 2012; revised 22 April 2012; accepted 23 April 2012; published online 13 June 2012

state using solid-state ^{1}H-NMR measurements.[12,13] Another series of PE reactor powders with normal molecular weights that were synthesized at different temperatures were also compared, based on the molecular motion of the crystalline and noncrystalline phases.[1] In both cases, the heating scan induces a remarkable reorganization of the crystalline phase with cooperative molecular motion of the noncrystalline phase, independent of sample molecular weight. Similar structural reorganization has been reported for ^{13}C-NMR analyses of UHMW-PE samples crystallized from solutions and melts.[14,15] In contrast, the structural change observed while heating highly drawn UHMW-PE fibers is limited in the crystalline phase, that is, transition from orthorhombic to hexagonal form.[16,17]

Indeed, a comparison of structural reorganization in UHMW-PE reactor powders with different morphologies has not been performed. Commercial UHMW-PE reactor powders are widely used in various applications, including in artificial knee cap implants, which require the direct sintering of UHMW-PE reactor powders at elevated temperatures. Therefore, the differences in the structural reorganization of commercial reactor powders examined in this study could be valuable information in optimizing such manufacturing processes. Rastogi *et al.*[4] reported that entanglement during the heating of reactor powders determines the resultant drawability of UHMW-PE materials. In this study, the structural characteristics of UHMW-PE powders were analyzed using a combination of DSC, SEM, TEM and solid-state NMR measurement techniques. The SEM and TEM observations allowed us to compare both the surface and internal morphologies of each reactor powder. In contrast, solid-state NMR analysis can distinguish the molecular motions of different phases, that is, crystalline and noncrystalline components, including the typical amorphous and intermediate components between crystalline and amorphous phases. Changes in solid-state NMR relaxation characteristics recorded upon heating were compared with corresponding DSC profiles. The data gathered from these various techniques suggest the development of unique structural characteristics of nascent UHMW-PE powders formed upon polymerization.

EXPERIMENTAL SECTION

Materials

Nine reactor powder samples were used in this work. Each powder has a viscosity average MW (M_v) range of several millions: Hifax 1900 from Hercules (USA), Hizex Million series (150M, 240S, 340M, 630M) from Mitsui Chemical (Japan), and Hostalen GUR series (4113, 4120, 4150, 4170) from Ticona (Germany). The molecular characteristics of these powders are listed in Table 1.

Measurements

These reactor powders were characterized by DSC measurements. The heating scans were performed from 80 to 180 °C at a heating rate of 10 °C min^{-1}. All of the scans were performed under an N_2 gas flow using a Perkin-Elmer (Waltham, MA, USA) Pyris 1 DSC. The sample T_m was evaluated by an onset ($T_{m,ons}$) and the peak positions ($T_{m,peak}$) of the endotherm. The fraction crystallinities were calculated from the heat of fusion (ΔH_f). An enthalpy value of 290 J g^{-1} was used as that of perfect crystals of PE.[18] These DSC characteristics were calibrated by indium and tin standards at each heating rate.

TEM observations of the rector powders were performed using a JEOL (Akishima, Japan) 1200EMX electron microscope operated at 80 kV. The samples were stained by RuO_4 vapor and embedded in epoxy resin. The assembly was cut into thin sections 60 nm thick using a Leica (Wetzlar, Germany) Reichert UltraCut S. microtome. SEM observations of the rector powders were performed using a Hitachi (Ibaragi, Japan) type S-5000 electron microscope operated at 5 kV.

NMR measurements were carried out using a JEOL MU-25 solid-state pulse NMR spectrometer at a resonance frequency of 25 MHz. The free induction decay (FID) was recorded by the solid-echo method.[19] Data collection was performed every 0.2 μs. The dead time before signal sampling was 2 μs. The measurement temperature was raised from room temperature to the temperature of complete sample melting. Before the signal sampling, the temperature was equilibrated isothermally for 5 min to obtain a homogeneous temperature distribution in the sample probe.

RESULTS AND DISCUSSIONS

DSC characteristics of reactor powders

The DSC traces of the UHMW-PE reactor powders examined in this study are depicted in Figure 1. Powders with the same range of MW, approximately 4×10^6, were selected. All of samples exhibit a single endotherm, approximately 140 °C. The Hifax 1900 and Hizex 340M powders showed similar sharp endotherms, whereas the Hostalen GUR4120 powder showed the opposite characteristics of the broadest endotherm. To examine the MW effect on the melting behavior of the UHMW-PE reactor powder samples, the series of Hostalen and Hizex grades were tested. The observed values of T_m, ΔH_f and calculated

Table 1 Molecular weight of UHMW-PE reactor powders used

Sample	M_v[a] /10^6	*Supplier*
Hifax 1900	4.0	Hercules
Hostalen GUR series		
4113	3.2	Ticona
4120	4.4	
4150	7.3	
4170	8.0	
Hizex million series		
150M	1.0	Mitsui Chemical
240S	2.0	
340M	3.5	
630M	6.0	

Abbreviation: UHMW-PE, ultra-high-molecular-weight polyethylene.
[a]Viscosity average MW.

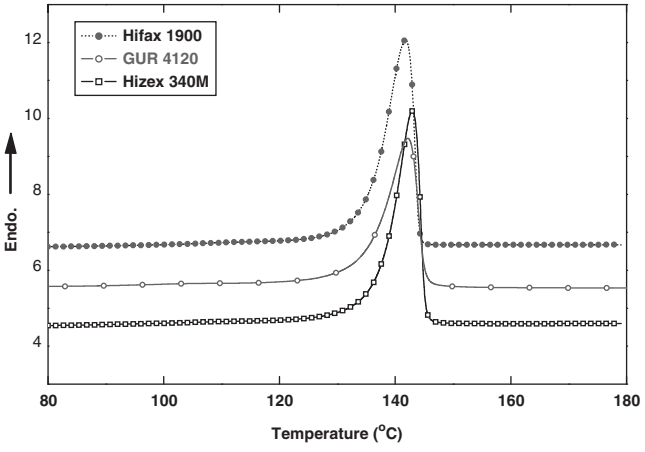

Figure 1 Comparison of DSC melting profiles scanned for reactor powders of UHMW-PE examined in this study. The observed heating rate was 10 °C min^{-1}.

crystallinity for these powder series are summarized in Table 2. Recognizable differences due to sample MW were not observed based on DSC melting characteristics.

Initial morphologies

The surface structure of the powders was characterized by SEM observations. Figure 2 shows images of two typical UHMW-PE powders, Hifax 1900 and Hostalen GUR4120, which had the highest and lowest crystallinities, respectively, as evaluated by DSC measurements. For the highly crystalline Hifax 1900 powder, the major structure consists of particles with a radius of several hundreds of nanometers. In the high-magnification image of this powder, the internal structure is also observable from the cracks on the surface. The outer surface is covered by a smooth, flat paste-like structure. In the case of the poorly crystalline Hostalen GUR4120 powder, the particle size is larger than that of the Hifax 1900 powder. Many fibrils are also observed between these particles. These fibrils have a diameter of around several tens of nanometers.

Table 2 DSC melting characteristics for UHMW-PE reactor powders used in this work

Sample	$T_{m,ons}$ (°C)[a]	$T_{m,peak}$ (°C)[b]	ΔH_f ($J g^{-1}$)[c]	*Crystallinity (%)*[d]
Hifax 1900	135.0	141.8	232.3	80.1
Hostalen GUR Series				
4113	129.9	140.8	202.5	69.8
4120	132.3	140.1	197.1	68.0
4150	134.7	142.2	199.4	68.8
4170	135.0	142.6	196.7	67.8
Hizex Million Series				
150M	133.4	140.8	211.3	72.9
240S	135.1	142.2	216.2	74.6
340M	137.0	142.9	224.2	77.3
630M	136.8	143.0	211.5	72.9

Abbreviations: DSC, differential calorimetry; HR, heating rate; UHMW-PE, ultra-high-molecular-weight polyethylene.
[a]Peak melting temperature ($T_{m,peak}$).
[b]Melting onset temperature ($T_{m,ons}$)
[c]Heat of fusion (ΔH_f) were evaluated from DSC melting profiles recorded at a HR of $10\,°C\,min^{-1}$.
[d]Crystallinity was calculated from the observed ΔH_f assuming that ΔH_f^o of the 100% orthorhombic crystal of PE is $290\,J\,g^{-1}$.

To examine the internal morphologies of these powders, both initial powders were observed directly by TEM. Figure 3 compares the sets of TEM images for the Hifax 1900 and Hostalen GUR4120 UHMW-PE powders. The TEM images are two-dimensional; thus, the fibrillar structure of the Hostalen GUR4120 powder shows a large free volume in Figure 3b. The internal crystalline morphology of each powder is emphasized in the high-magnification images. The area of each crystalline region is much larger for Hifax 1900 than for Hostalen GUR4120. Furthermore, the crystalline/amorphous arrangements of the two powders are quite different from each other. These two components are randomly distributed within the particles of the Hifax 1900 powder, forming a kind of domain network structure, but the Hostalen GUR4120 powder shows a lamellar-like crystal/amorphous phase arrangement.

The morphologies of the Hizex family were similar to those of Hifax 1900. These morphological features for specific powder series were not influenced by sample MW.

^{1}H-NMR relaxation for initial powders

The as-polymerized powder morphology reflects the initial relaxation behavior evaluated by solid-state ^{1}H-NMR measurements. Figure 4 compares the ^{1}H-NMR FID profiles for UHMW-PE reactor powders having the same range of MW, approximately 4×10^6. These FIDs were recorded at room temperature. The peaks of these profiles,

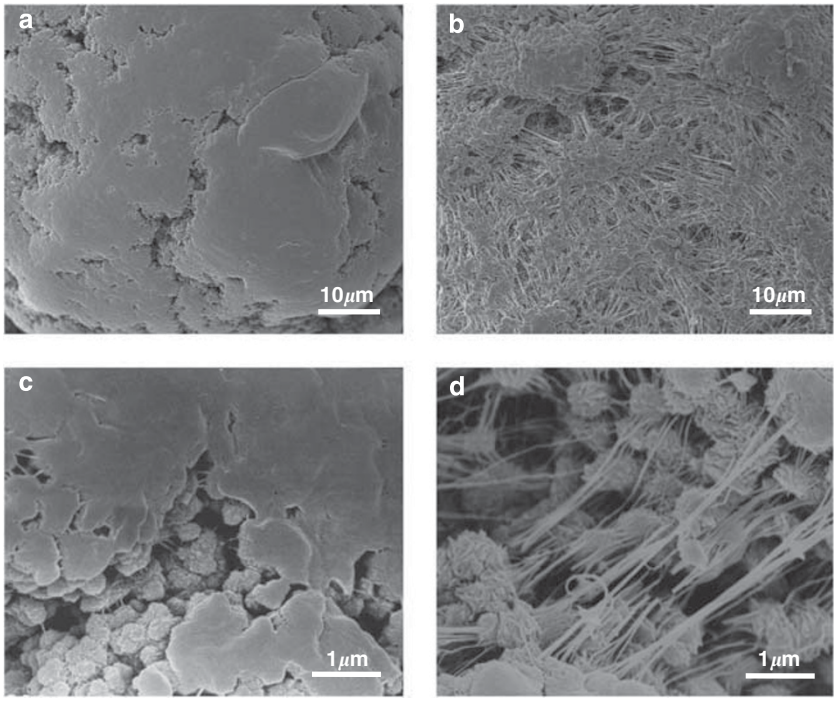

Figure 2 SEM images of Hifax 1900 (**a**, **c**) and Hostalen GUR4120 (**b**, **d**) UHMW-PE reactor powder samples. The top and bottom views correspond to low- and high-magnification images, respectively.

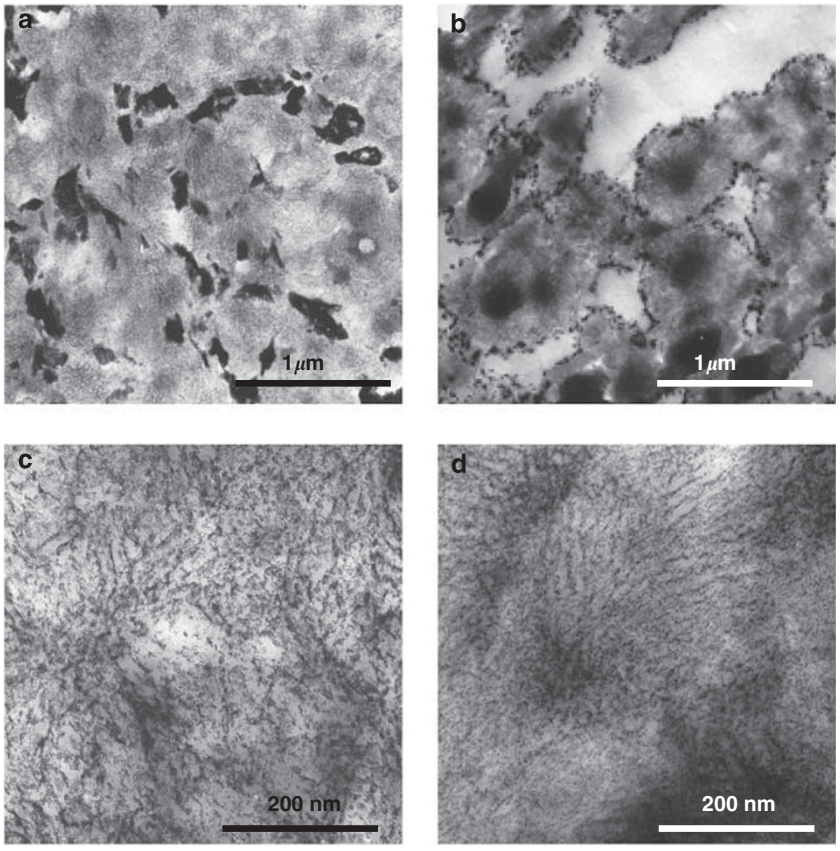

Figure 3 TEM images of Hifax 1900 (**a**, **c**) and Hostalen GUR4120 (**b**, **d**). The top and bottom views correspond to low- and high-magnification images, respectively.

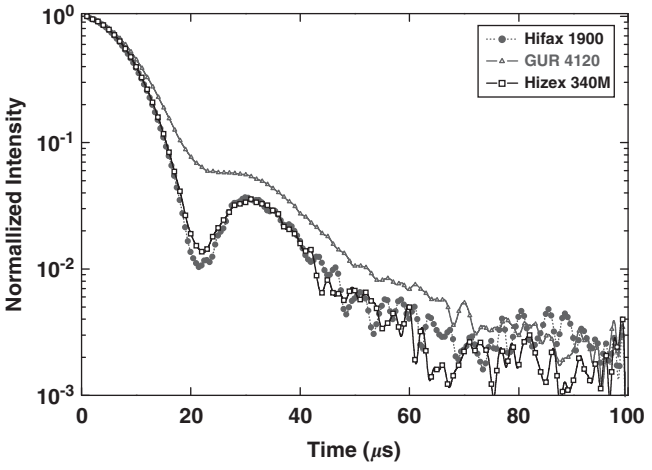

Figure 4 Comparison of ^{1}H-NMR FIDs observed at room temperature for the UHMW-PE reactor powders examined in this study.

Table 3 Summarized spin-spin relaxation characteristics of components resolved from FID observed at room temperature for UHMW-PE reactor powders[a]

Sample	*Crystalline $T_{2,ons}$ (μs)*	*Intermediate T_2 (μs)*	*Amorphous T_2 (μs)*
Hifax 1900	14.7 (82.3%)	25.0 (17.7%)	—
Hostalen GUR Series			
4113	15.2 (76.9%)	31.2 (22.3%)	64.3 (0.8%)
4120	15.6 (75.7%)	32.8 (24.3%)	—
4150	15.7 (77.6%)	32.4 (22.4%)	—
4170	15.4 (77.7%)	30.4 (20.2%)	47.9 (2.1%)
Hizex Million Series			
150M	14.7 (78.4%)	30.9 (20.4%)	52.5 (1.2%)
240S	14.7 (79.5%)	30.0 (19.5%)	50.1 (1.0%)
340M	14.7 (81.4%)	29.2 (18.3%)	66.4 (0.4%)
630M	15.1 (80.7%)	30.5 (19.3%)	—

Abbreviation: FID, free induction decay; UHMW-PE, ultra-high-molecular-weight polyethylene.
[a]Value in parentheses represents component ratio for corresponding relaxation.

which show a combination of drops in intensity and subsequent recovery, are clearly observed in the 20–30 μs region of these FIDs, especially for the highly crystalline Hifax 1900 powder. In contrast, this peak does not show any sharp drop for the amorphous-rich Hostalen GUR4120 powder. The profile of the Hizex Million 340M powder is similar to that of the highly crystalline Hifax 1900 powder because of their comparable crystallinities (see Table 3) and powder morphology. A comparison at a longer time scale beyond 100 μs does not reveal meaningful differences between the UHMW-PE powders examined in this study.

These FID profiles should contain at least two components, that is, the relaxations of crystalline and amorphous phases. The intermediate phase between the two components is often necessary for better

fitting. For this curve-resolution procedure, a Gauss/Sine function was assumed for the crystalline relaxation.[16] On the other hand, an amorphous FID was always reproduced by a typical exponential decay function. The intermediate component is represented by a Weibull function.[12] For characterization of the UHMW-PE reactor powders, a companion of these different relaxation curves enabled us to evaluate the component fractions and molecular motions in each phase. Corresponding curve-fitting results at different temperatures for Hifax 1900 are depicted in Figure 5. The Gauss/Sine function exhibits a wavy shape, showing a steep intensity decay to negative values at the early stage of the decay. Such a negative value for the crystalline component often disappears in the log plots in the time region of 15–30 μs, as shown in Figure 5a. The relaxation characteristics obtained by such a curve-fitting procedure are summarized in Table 3. Depending on the powder, the amorphous component was omitted in the FID curve fitting. Here, the spin–spin relaxation time (T_2) was defined as the reciprocal of the integral width of the corresponding broad-line spectrum on the frequency scale. Detailed calculations for this analysis are described elsewhere.[13] The fraction of the crystalline component, which corresponds to the sample crystallinity, was the highest for the Hifax 1900 reactor powder, which agrees well with the DSC data shown in Figure 1 and Table 2. The crystalline T_2 was slightly shorter for the poorly crystalline Hostalen GUR4120 powder, suggesting constrained crystalline chain motions. Regarding intermediate relaxation, the shortest T_2 was obtained for the highly crystalline Hifax 1900 powder due to restricted chain motion. Both the crystalline and intermediate relaxation characteristics for the Hizex powder series are more similar to those of the Hifax 1900 powder, which shows the same range of crystallinity (~80%), than to those of the Hostalen GUR series, which shows lower crystallinity.

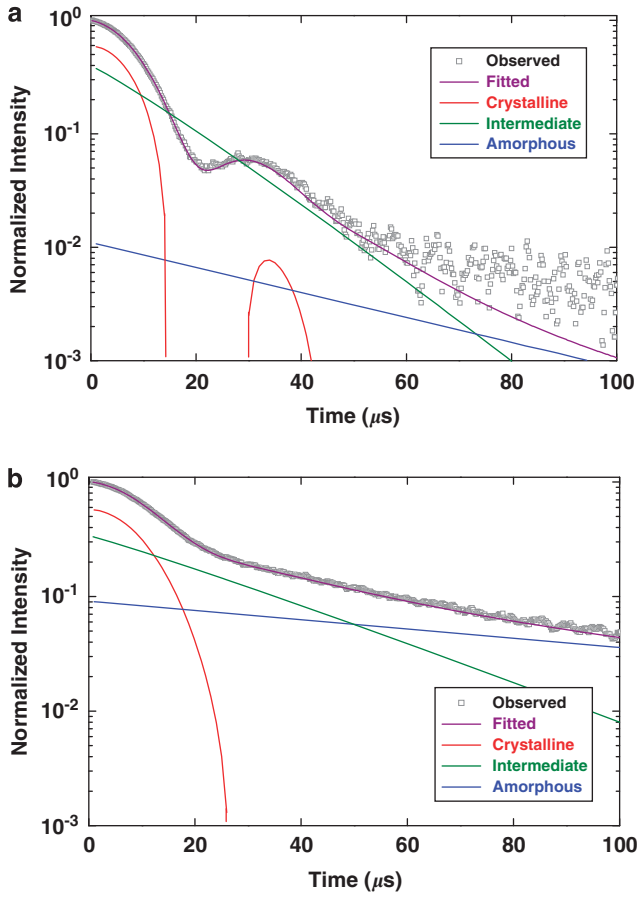

Figure 5 Curve-fitting results for the FID profile recorded for Hifax 1900 at 60 °C (**a**) and 130 °C (**b**), assuming crystalline (Gauss/Sine function), intermediate (Weibull function) and amorphous components (exponential function).

Relaxation changes during heating

These differences in the relaxation characteristics among the powders were further investigated by changes in the FID profiles during heating. Figure 6 compares the FID profiles recorded at various temperatures for the Hifax 1900 reactor powder. Gradual heating depresses the crystalline peak in the FIDs, which ultimately disappears approximately 120 °C. The profile intensity at longer times beyond 50 μs also increases with temperature owing to accelerated amorphous and/or intermediate molecular motions. The FID changes upon heating the other powder series were also recorded.

The FID profiles observed at any temperature could be fitted by three-component functions featuring crystalline, intermediate and amorphous components, independent of the powder series. To evaluate both the integral width and component ratio for the crystalline and amorphous phases, a Fourier-transformation procedure was applied to the resolved profiles.[12] The obtained integral width is plotted in Figure 7. A small integral width indicates a high T_2 and thus reduced molecular motion in the crystalline components. Changes in the crystalline integral width during heating can be used to classify the targeted powders well. All powders exhibited a reduction in crystalline integral width with increasing temperature, that is, (1) nearly constant values were observed from room temperature to the critical temperature, (2) the values rapidly decreased beyond this critical temperature up to the temperature of sample melting, and (3) saturated reduction was observed in the melt.

The temperature where the relaxation of the crystalline component begins corresponds to the so-called α_c-relaxation temperature.[20] As discussed in our previous study,[13] the rapid reduction of the crystalline integral width beyond this critical temperature indicates

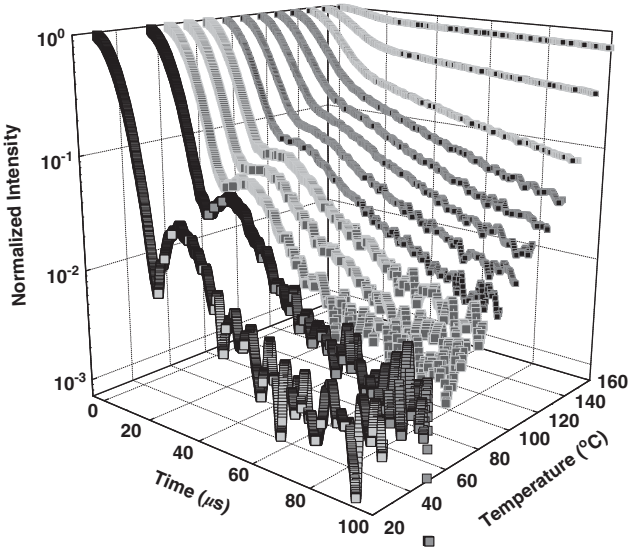

Figure 6 Changes in the FIDs during heating for highly crystalline Hifax 1900 reactor powder.

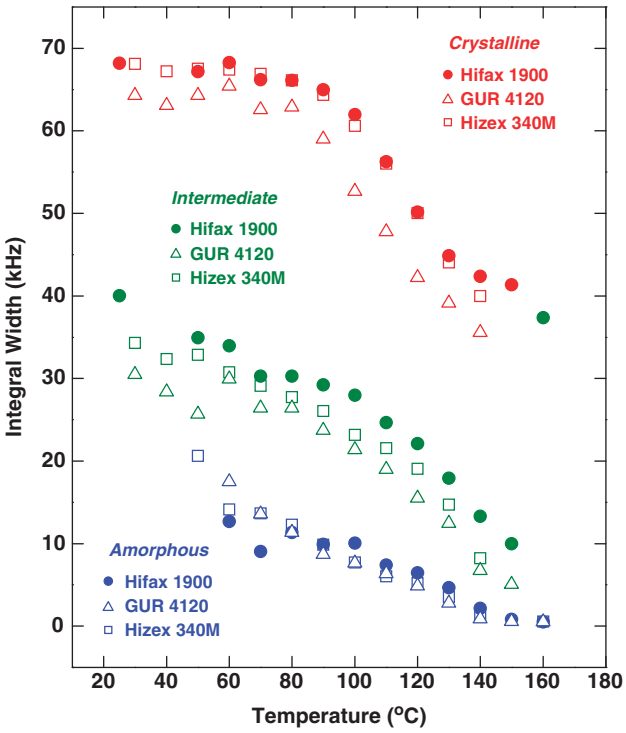

Figure 7 Temperature dependencies of integral widths during heating for the UHMW-PE reactor powders examined in this study. Changes in both values for crystalline, intermediate and amorphous relaxations were plotted for each sample.

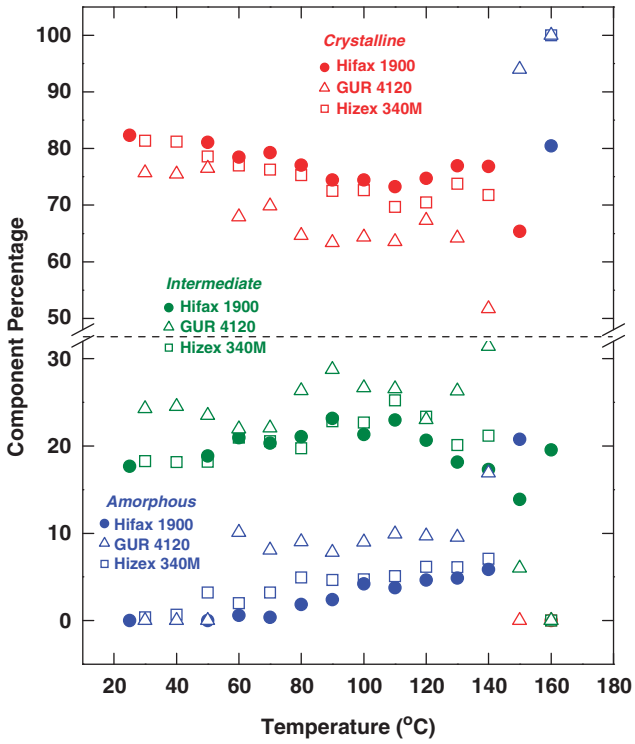

Figure 8 Temperature dependencies of component percentages during heating for the UHMW-PE reactor powders examined in this study. Changes in both values for crystalline, intermediate and amorphous relaxations were plotted for each sample.

the sudden release of crystalline chain motion during heating for solution-crystallized UHMW-PE samples. Rastogi *et al.*[21] also reported that remarkable lamellar thickening occurs above such a critical temperature. According to previous solid-state ^{13}C-NMR studies for low and high MW-PEs,[22,23] a 180° screw jump rotation along the chain axis occurs in the crystalline region at the α_c-relaxation temperature, and chains can diffuse between the crystalline and amorphous regions. Such diffusional movement may contribute to the lamellar thickening.

In this study, the highly crystalline Hifax 1900 powder exhibited a higher integral width in the crystalline phase than the poorly crystalline Hostalen GUR4120 powder. The plots for the Hizex powder series are nearly identical to those for the Hifax 1900 reactor powder, exhibiting restricted molecular motion in the crystalline phase. Additionally, the critical temperature accompanying the decreases in the crystalline integral width is higher for the highly crystalline Hifax 1900 powder.

In contrast, both the intermediate and amorphous relaxations exhibit a continuous decrease in integral width, independent of the tested powder, as shown in Figure 7. In case of the intermediate phase, the highest integral widths were always obtained for Hifax 1900, which is similar to the trend observed for the crystalline integral width described above. However, the integral width of the amorphous component is independent of the powder. These results suggest that the chain mobility of the intermediate components is restricted by the adjacent crystalline component, but the amorphous region is free even in the initial state before heating.

The changes in the fractions of crystalline, intermediate and amorphous phases during heating were also estimated from the above FID resolutions. The obtained percentage values are plotted as a function of temperature in Figure 8. The corresponding DSC melting behavior for the powders shown in Figure 1 could be compared with these crystallinity changes evaluated by ^{1}H-NMR profile analyses. The highest crystallinity was always obtained for the Hifax 1900 powder, independent of temperature. However, the amount of amorphous component was almost zero for all of the powders. In fact, the initial reactor powers were composed of an intermediate component as well as a crystalline component. This is similar to the composition of solution-crystallized UHMW-PE, but different from that of melt-crystallized UHMW-PE containing 10% amorphous with 30% intermediate components.[12] The amount of amorphous component gradually increases with increasing temperature, but remains 5% even at 140 °C. In contrast, the crystalline component percentage exhibits (1) a slight decrease from room temperature to the critical temperature, (2) followed by an upward recovery and (3) a final decrease in the completely amorphous state, independent of the powder type. This three-step change in the component percentage coincides with that of the integral widths in Figure 7. These results indicate that a combination of restricted crystalline chain motions at low temperatures and the rapid release of these motions at the corresponding critical temperature is the origin of the above-mentioned change in crystallinity. The other change in the intermediate component mainly reflects that of the crystalline component.

Mechanism of structural change during heating

The origins of these phase changes could be speculated to be the following. At the early stage of gradual heating, the intermediate components located between the amorphous/crystalline components

relax. Such a release of the intermediate component induces a gradual transition from the crystalline to the intermediate phase; thus, the fraction of the crystalline component decreases with increasing temperature from room temperature to the critical temperature. However, the molecular motion of the majority of crystalline chains, which are located inside crystalline domains, is still restricted. Therefore, a constant crystalline integral width was maintained over this temperature range. Beyond the critical temperature, these relaxed chains participate in reorganization during heating, allowing for the gradual recovery of the crystalline component fraction, which was not detected by the DSC profiles shown in Figure 1. Dynamic cooperative chain motions in the crystalline and intermediate components accelerate the relaxation of crystalline chains, resulting in the rapid decrease in the integral width. Further heating ultimately leads to sample melting, where the crystalline spectrum gradually disappears.

The assignment of the fibrillar structure of the Hostalen powder is also of interest. This structure is formed by internal expansion stress during polymerization,[24,25] Because the intermediate component also exhibits restricted molecular motion, the characteristics of this component and those of the fibrillar structure are similar. However, this assignment requires further supporting data, such as the morphological changes that occur while heating the reactor powder. This is left as a subject for future study of the detailed morphological assignments of the UHMW-PE reactor powders.

CONCLUSIONS

UHMW-PE reactor powders have characteristic surface and internal morphologies that are quite different from those of the typical spherulite structure of melt-crystallized samples and those of regular lamellar stacking structures for solution-crystallized samples. The powders were composed of particles with radii measuring several hundreds of nanometers. Some powders featured fibrils tied between these particles. In such particles, a crystalline domain network or lamellar-like structure could be recognized, depending on the powder series. ^{1}H-NMR FID profiles, particularly the changes in the profiles during heating, revealed the different relaxation components of the powders studied, which reflected the amount of these unique morphological units in each powder. On the basis of this combination of the integral width and intensity changes, the powder series examined in this study could be classified into two categories. In the first category, typically represented by the Hifax 1900 reactor powder, the domain network structure prevents crystalline chain relaxation from room temperature to approximately 90 °C. In contrast, the lamellar-like structure of the Hostalen GUR series powders shifts this limitation on crystalline chain motion to lower temperatures. The Hizex powders exhibit relaxation changes similar to those of the Hifax 1900 powders. However, the crystallinity change observed upon heating showed the same trend for all powder series: (1) decrease up to the critical temperature, (2) subsequent recovery due to structural reorganization, and (3) drastic decrease induced by complete melting. This three-step change in crystallinity during heating is not detectable by typical DSC measurements. Such crystalline relaxation is induced by the enhanced molecular motion of the intermediate component between the crystal/amorphous phases.

ACKNOWLEDGEMENTS

This work was partly supported by the Industrial Technology Research Grant Program from the New Energy and Industrial Technology Development Organization (NEDO) of Japan and the Ogasawara Science Foundation.

1 Uehara, H., Uehara, A., Kakiage, M., Takahashi, H., Murakami, S., Yamanobe, T. & Komoto, T. Solid-state characterization of polyethylene reactor powders and their structural changes upon annealing. *Polymer* **48,** 4547 (2007).
2 Patil, N., Balzano, L., Portale, G. & Rastogi, S. A study on the chain–particle interaction and aspect ratio of nanoparticles on structure development of a linear polymer. *Macromolecules* **43,** 6749 (2010).
3 Talebi, S., Duchateau, R., Rastogi, S., Kaschta, J., Peters, G. W. M. & Lemstra, P. J. Molar mass and molecular weight distribution determination of UHMWPE synthesized using a living homogeneous catalyst. *Macromolecules* **43,** 2780 (2010).
4 Rastogi, S., Lippits, D. R., Peters, G. W. M., Graf, R., Yao, Y. & Spiess, H. W. Heterogeneity in polymer melts from melting of polymer crystals. *Nature Mat.* **4,** 635 (2005).
5 Lippits, D. R., Rastogi, S., Höhne, G. W. H., Mezari, B. & Magusin, P. C. M. M. Heterogeneous distribution of entanglements in the polymer melt and its influence on crystallization. *Macromolecules* **40,** 1004 (2007).
6 Lippits, D. R., Rastogi, S., Talebi, S. & Bailly, C. Formation of entanglements in initially disentangled polymer melts. *Macromolecules* **39,** 8882 (2006).
7 Kanamoto, T., Ohama, T., Tanaka, K., Takeda, M. & Porter, R. S. Two-stage drawing of ultra-high molecular weight polyethylene reactor powder. *Polymer* **28,** 1517 (1987).
8 Uehara, H., Kanamoto, T., Kawaguchi, A. & Murakami, S. Real-time x-ray diffraction study on two-stage drawing of ultra-high molecular weight polyethylene reactor powder above the static melting temperature. *Macromolecules* **29,** 1540 (1996).
9 Uehara, H., Nakae, M., Kanamoto, T., Ohtsu, O., Sano, A. & Matsuura, K. Structural characterization of ultra-high molecular weight polyethylene reactor powders based on fuming nitric acid etching. *Polymer* **39,** 6127 (1998).
10 Rastogi, S., Yao, Y., Ronca, S., Bos, J. & van der Eem, J. Unprecedented high-modulus high-strength tapes and films of ultrahigh molecular weight polyethylene via solvent-free route. *Macromolecules* **44,** 5558 (2011).
11 Uehara, H., Yoshida, R., Kakiage, M., Yamanobe, T. & Komoto, T. Continuous film processing from ultra-high molecular weight polyethylene reactor powder and mechanical property development by melt-drawing. *Ind. Eng. Chem. Res.* **45,** 7801 (2006).
12 Uehara, H., Yamanobe, K. & Komoto, T. Relationship between solid-state molecular motion and morphology for ultra-high molecular weight polyethylene crystallized under different conditions. *Macromolecules* **33,** 4861 (2000).
13 Uehara, H., Aoike, T., Yamanobe, T. & Komoto, T. Solid-state ^{1}H-NMR relaxation analysis of ultra-high molecular weight polyethylene reactor powder. *Macromolecules* **35,** 2640 (2002).
14 Kuwabara, K., Kaji, H., Tsuji, M. & Horii, F. Crystalline-noncrystalline structure and chain diffusion associated with the 180° flip motion for polyethylene single crystals as revealed by solid-state ^{13}C NMR analyses. *Macromolecules* **33,** 7093 (2000).
15 Yao, Y.-F., Graf, R., Spiess, H. W. & Rastogi, S. Restricted segmental mobility can facilitate medium-range chain diffusion: a NMR study of morphological influence on chain dynamics of polyethylene. *Macromolecules* **41,** 2514 (2008).
16 Hu, W.-G., Boeffel, C. & Schmidt-Rohr, K. Chain flips in polyethylene crystallites and fibers characterized by dipolar ^{13}C NMR. *Macromolecules* **32,** 1611 (1998).
17 Kuwabara, K. & Horii, F. Solid-state ^{13}C NMR analyses of the orthorhombic-to-hexagonal phase transition for constrained ultradrawn polyethylene fibers. *Macromolecules* **33,** 5600 (1999).
18 Wunderlich, B. & Cormier, C. M. Heat of fusion of polyeetheyene. *J. Polym. Sci. Polym. Pt. A-2* **5,** 987 (1967).
19 Gao, P., Cheung, M. K. & Leung, T. Y. Effects of compaction pressure on cohesive strength and chain mobility of low-temperature compacted nascent UHMWPE. *Polymer* **37,** 3265 (1996).
20 Hu, W.-G. & Schmidt-Rohr, K. Polymer ultradrawability: the crucial role of α-relaxation chain mobility in the crystallites. *Acta. Polym.* **50,** 271 (1999).
21 Rastogi, S., Spoelstra, A. B., Goossens, J. G. P. & Lemstra, P. J. Chain mobility in polymer systems: on the borderline between solid and melt. 1. lamellar doubling during annealing of polyethylene. *Macromolecules* **30,** 7880 (1997).
22 Schmidt-Rohr, K. & Spiess, H.W. Chain diffusion between crystalline and amorphous regions in polyethylene detected by 2d exchange ^{13}C NMR. *Macromolecules* **24,** 5288 (1991).
23 Kuwabara, K., Kaji, H. & Horii, F. Solid-state ^{13}C NMR analyses for the structure and molecular motion in the relaxation temperature region for metallocene-catalyzed linear low-density polyethylene. *Macromolecules* **33,** 4453 (2000).
24 Keller, A. & Willmouth, F. M. On the morphology and origin of the fibres observed in nascent Ziegler polyethylene. *Makromol. Chem.* **121,** 42 (1969).
25 Chanzy, H. D., Revol, J. F., Marchessault, R. H. & Lamandé, A. Nascent Structures during the polymerization of ethylene i. morphology and model of growth. *Kolloid-Z. Z* **251,** 563 (1973).